ARTICLE

Cytosolic delivery of quantum dots mediated by freezing and hydrophobic polyampholytes in RAW 264.7 cells

Received 00th January 20xx,
Accepted 00th January 20xx

DOI: 10.1039/x0xx00000x

Sana Ahmed[a, b], Tadashi Nakaji-Hirabayashi[b, c] Robin Rajan[a], Dandan Zhao[a] and Kazuaki Matsumura*[a]

Quantum dots (QDs) can be delivered efficiently inside macrophages using a freeze-concentration approach. In this study, we introduced a new, facile, high concentration-based freezing technology of low toxicity. We also developed QD-conjugated new hydrophobic polyampholytes using poly-L-lysine (PLL), a naturally derived polymer, which showed sustained biocompatibility, stability over one week, and enhanced intracellular delivery. When freeze-concentration was applied, the QD-encapsulated hydrophobic polyampholytes showed a higher tendency to adsorb onto the cell membrane than the non-frozen molecules. Interestingly, we observed that the efficacy of adsorption of QDs on RAW 264.7 macrophages was higher than that on fibroblasts. Furthermore, the intracellular delivery of QDs using hydrophobic polyampholytes was higher than those of PLL and QDs. *In vitro* studies revealed the efficient endosomal escape of QDs in the presence of hydrophobic polyampholytes and freeze-concentration. Collectively, these observations indicated that the promising combination of freeze-concentration and hydrophobic polyampholytes may act as an effective and versatile strategy for the intracellular delivery of QDs, which can be used for biological diagnosis and therapeutic applications.

Introduction

Currently, the interest in fluorescent tags for tracking biological processes such as protein-protein interactions and signalling, as well as for imaging of tissues and cells, is increasing. In this context, the applicability of quantum dots (QDs) in biological systems has attracted considerable attention because of their brightness and photo-stable property, which can be used to investigate single molecule dynamics *in vitro*.[1] Furthermore, QDs are used as photosensitizers in photodynamic therapy owing to their energy donation capability, ability to label cellular proteins and act as visible drug carriers, sensitivity in cellular imaging, and suitability for *in vivo* imaging.[2] In addition, numerous studies have investigated the delivery of QDs into the cytoplasm for studying protein dynamics. [3,4]

However, the delivery of QDs across the plasma membrane remains challenging because of their size and surface charge.[5] To overcome this issue, several physical strategies have been used to deliver QDs efficiently inside cells. Electroporation is one such method, which favours the introduction of QDs into cells.[6] However, the cell damage associated with external electric pulses across the cell membrane impedes their further use.[7] Various studies have reported the use of electroporation-induced non-endocytic pathways, which results in higher oxidation stress and finally cell death.[8] In many ways, endocytic pathways are more favourable, as they are considered to be the active transport mechanism that increases molecular interaction between cells and nanoparticles, which can be utilised for targeting, uptake, and intracellular trafficking with efficient cellular response.[9] Therefore, development of a new strategy that can increase the interaction between cells and nanomaterials and favour endocytosis is required.

In 2014, our group pioneered the development of a unique freeze-concentration-mediated method of delivering nanomaterials.[10-15] Freeze-concentration is a physical approach that focuses on enhancing the concentration of materials at extremely low temperature. The formation of ice crystals at very low temperatures ejected the protein-nanocarrier complexes, which eventually increased their concentration. In this study, we used the freeze-concentration method for inducing endocytic transportation of macromolecules such as proteins and genes inside cells for gene therapy and immunotherapy. This advanced technique was cost-

[a]School of Materials Science, Japan Advanced Institute of Science and Technology (JAIST), Nomi, Ishikawa 923-1292, Japan E-mail: mkazuaki@jaist.ac.jp
[b]Graduate School of Science and Engineering, University of Toyama, 3190 Gofuku, Toyama, Toyama 930-8555, Japan
[c]Graduate School of Innovative Life Science, University of Toyama, 3190 Gofuku, Toyama, Toyama 930-8555, Japan

Electronic Supplementary Information (ESI) available: [details of any supplementary information available should be included here]. See DOI: 10.1039/x0xx00000x

effective and simple, and suitable for intracellular delivery of candidate cargoes.

Although the physical methodology is an effective approach for inducing internalization of macromolecules, stability and potential toxicity remain critical issues for its application in *in vitro* model systems.[16] Hence, nanocarriers are being increasingly used for safe delivery. Therefore, in our previous studies, we focused on developing not only a physical methodology but also a self-assembled polyampholyte-based nanoparticle as a carrier.[10-15] Polyampholyte nanoparticles are delivered efficiently into live cells via endocytosis, and combined with the freeze-concentration method, the intracellular uptake of protein-conjugated polyampholyte nanoparticles was superior to those of conventional carriers such as bare liposomes.[11]

Furthermore, cell specific-imaging is important for correct diagnosis and cell-directed therapies.[17] Macrophages play important roles in inflammatory reactions and innate immune response to pathogens and are also involved in tissue regeneration.[18] Upon activation, macrophages mediate various biological effects such as specific inflammatory as well as immune responses that are involved in the development of several diseases. [19]

The present study aimed to evaluate the intake of QDs by combining the freezing strategy with the use of hydrophobic polyampholytes in RAW 264.7 macrophages. Our observations will improve basic understanding regarding intracellular delivery of QDs and provide a promising combination for imaging of cells and biomolecules **(Scheme 1)**.

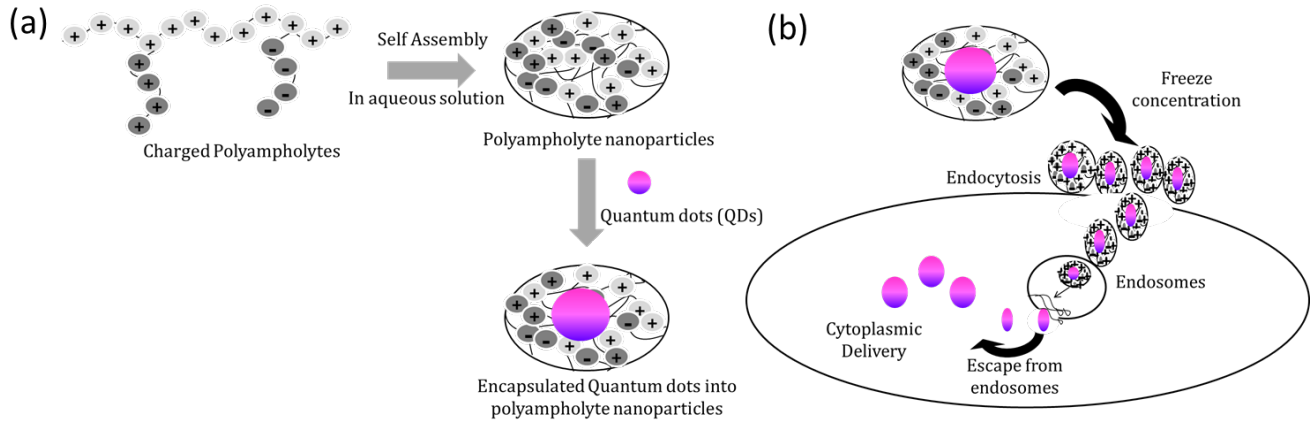

Scheme 1 Schematic representation showing the delivery of quantum dots (QDs) using polyampholyte nanoparticles and freeze-concentration. (a) Preparation of polyampholyte nanoparticles loaded with QDs. (b) Internalization of polyampholyte-loaded QDs inside cells via the freezing method.

Experimental

Reagents

QD® 655 streptavidin conjugate (1 µM solution in 1 M betaine, 50 mM borate, pH 8.3, with 0.05% sodium azide) was purchased from Thermo Fischer Scientific (Waltham, MA, USA), 25% (w/w) ε-Poly-L-lysine (PLL) was purchased from JNC Corp. (Yokohama, Japan), and LysoTracker Green DND-26 and Hoechst 33342 were purchased from Molecular Probes Inc. (Eugene, OR, USA). Dodecylsuccinic anhydride (DDSA) was purchased from Wako Pure Chemicals Industries Ltd. (Osaka, Japan) and fluorescein isothiocyanate (FITC) was from Sigma Aldrich (St Louis, MO, USA). Cryoscarless (dimethyl sulfoxide (DMSO)-free) was purchased from Funakoshi, Co. Ltd. (Bunkyo-ku, Tokyo, Japan)

Preparation of hydrophobic polyampholyte nanoparticles

Hydrophobic polyampholytes were prepared as described in our previous studies. Briefly, PLL was reacted with hydrophobic succinic anhydride (DDSA; 10 mol %) at 100 °C for 2 h with constant stirring. Furthermore, the polyampholytes were characterized using ^{1}H and ^{13}C nuclear magnetic resonance (NMR) spectroscopy at 25 °C on a Bruker AVANCE III 400 spectrometer (Bruker Biospin Inc., Switzerland) in methanol-d_4. The degree of substitution of DDSA was obtained by 2D NMR and the following equation.

Degree of substitution for DDSA (%) = $(2*A_{\delta 0.89}/3A_{\delta 1.47\text{-}1.62})*100$

In addition, polyampholytes were characterized by attenuated total reflectance Fourier transform infrared (ATR-FTIR). The dried polymers were mounted on the ZnSe crystal on the single-reflection ATR accessory (JASCO ATR PRO450-S), and the spectra were obtained using a JAFCO FT/IR-4200 system.

Preparation of QD- polyampholyte nanoparticle complex

Polyampholyte nanoparticles were suspended in phosphate-buffered saline (PBS) (–) at 1 mg/mL. Then, the appropriate amount of QDs (25 nM) was mixed and incubated for 30 min at room temperature.

Hydrodynamic size and zeta potential

Size distribution, stability, and surface charge were measured using the dynamic light scattering (DLS) technique with a Zeta sizer 3000 (Malvern Instruments, Worcestershire, UK) at a scattering angle of 135° at 25 °C. The nanoparticles were dispersed in PBS without

calcium and magnesium [PBS (–)], and the zeta potential was measured using the default parameters (dielectric constant of 78.5, refractive index of 1.6).

Morphological analysis

The morphology of the QD and QD-polyampholyte complex was detected using a Hitachi H-600 transmission electron microscope (TEM) operated at an accelerating voltage of 100 kV. A drop of the QD or QD-polyampholyte complex was placed on a copper grid (200 mesh covered with carbon) and allowed to dry for 10 min prior to the measurement.

Preparation of FITC-labelled polyampholytes

Polyampholyte nanoparticles were labelled with the fluorescent FITC dye. For labelling, 25% (w/w) aqueous PLL was reacted with FITC at a 1/10,000 molar ratio for 24 h at room temperature. The resultant solution was purified via dialysis (molecular weight cut-off 3 kDa) against water for 3 days.[10, 11] After labelling, the same procedure was used for the preparation of hydrophobically modified polyampholytes as described above.

Cell culture

Murine RAW 264.7 macrophage cells (American Type Culture Collection, Manassas, VA, USA) were cultured in Dulbecco's modified Eagle's medium (DMEM; Sigma Aldrich) supplemented with 10% foetal bovine serum (FBS) at 37 °C in a 5% CO_2 humidified atmosphere. When the cells reached 60% confluence, they were sub-cultured after trypsinisation with 0.25% (w/v) trypsin containing ethylenediamine tetraacetic acid (EDTA) in PBS (–) and seeded onto new tissue-culture plates.

Cytotoxicity of hydrophobic polyampholytes

Cytotoxicity was determined using the 3-(4,5-dimethyl thial-2yl)-2,5-diphenyltetrazalium bromide (MTT) assay.[10, 11] RAW 264.7 macrophages (1×10^3 cells/mL) were cultured in each well and incubated under saturating humidity conditions at 37 °C in the presence of 5% CO_2. After 72 h of incubation at 37 °C, 0.1 mL media containing different concentrations of QDs were added, followed by addition of 1 mg/mL hydrophobic polyampholytes (constant concentration) to the cells and incubation for 24 h. Then, MTT solution (0.1 mL, 300 µg/mL in medium) was added to the cells. The cells were incubated for 4 h at 37 °C. After incubation, the solutions were removed, replaced by DMSO (100 µL), and allowed to stand for 15 min to allow completion of the reaction. The resulting colour intensity was measured using a microplate reader (Versa Max, Molecular Devices Co., Sunnyvale, CA, USA) at 540 nm, which was proportional to the number of viable cells. Toxicity was measured as the concentration of the compound that caused a 50% reduction in MTT uptake by a treated cell culture compared to the untreated control culture (IC_{50}).

Adsorption of polyampholyte-QD conjugates in macrophage and fibroblast cell lines using the freezing procedure

RAW 264.7 macrophages were counted and resuspended at a density of 1×10^6 cells/mL in 10% cryoscarless DMSO-free cryoprotectant containing 50 µL of polyampholyte nanoparticles conjugated with QDs (comprising 0.25 nM of QDs in 1 mg/mL of polyampholyte nanoparticles). This mixture was added in 1.9 mL cryo-vials (Nalgene, Rochester, NY) and placed in a controlled freezing container with a cooling rate of 1 C/min, which was subsequently stored overnight in a −80 °C deep freezer (Nihon freezer). Next day, the vials containing cells and polyampholyte-QDs were thawed at 37 °C and washed thrice with DMEM. To assess cell viability, the cells were counted on a haemocytometer using the trypan blue staining method. Cell viability was determined as the number of viable cells divided by the total number of cells. Furthermore, the adsorption of polyampholyte-QDs to the cells was observed using a confocal laser scanning microscope (CLSM, FV-1000-D; Olympus, Tokyo, Japan). An argon laser (543 nm) was used to excite the QD. The emitted fluorescence was detected using the 633 nm long-pass filter.

Internalization of polyampholyte-QD conjugates using freeze concentration

After thawing and washing thrice with DMEM, the cells were seeded in a 35-mm glass-bottomed dish and incubated for 24 h to allow cell attachment. After incubation for 24 h, the attached cells were washed with PBS and internalization of polyampholyte-QDs was observed using CLSM.

Endosomal escape of quantum dots

A thawed suspension of 1×10^4 cells/mL of RAW 264.7 cells containing 10% cryoscarless DMSO-free cryoprotectant with PLL-DDSA(10)-QDs (comprising 0.25 nM QDs in 1 mg/mL of PLL-DDSA(10)) were seeded onto a glass-bottomed dish. The cells were incubated for 24 h in a 5% CO_2 humidified atmosphere at 37 °C. Lysotracker Green DND-26 and Hoechst dye 33342 were added, and the cells were further incubated for 30 min prior to observation. The samples were rinsed with PBS and observed using CLSM.

Statistical analysis

All data are expressed as means ± standard deviation (SD). All experiments were conducted in triplicate. To compare data, one-way analysis of variance (ANOVA) with post-hoc Fischer's protected least significant difference test was used. Differences were considered statistically significant at $P < 0.05$.

Results and Discussions

Preparation of hydrophobic polyampholyte

The advantages associated with the cytoplasmic delivery of QDs are their selective targeting, live cell monitoring, and tracking of

cytoplasmic processes. However, owing to the potential toxicity associated with QDs, many researchers do not use QDs alone for treating patients. The use of nanocarriers considerably reduces toxicity. An ideal nanocarrier should show good biocompatibility, low toxicity, and high stability. Previously, Ishihara et al. have used a polymer consisting of 3-methacryloyloxyethyl phosphorylcholine (MPC), which enables the delivery of QDs made of semiconducting materials into cells.[20] In another study, Fukui et al. have used the nanogels of cholesterol-bearing pullulan modified with amino groups for introducing QDs to periodontal ligament cells.[21]

Here, we developed a new amphiphilic self-assembled hydrophobic polyampholyte by randomly modifying hydrophobic succinic anhydride such as DDSA (10 mol %) into ε-PLL to form PLL-DDSA (**Scheme 2**). Using ^{1}H NMR analysis, we successfully characterized the modification of DDSA into PLL (**Fig. S1)**. Furthermore, the resulting substitution of DDSA in ε-PLL was 9.1% (calculated using the equation mentioned in the Experimental section) **(Fig. S1**). Moreover, the ATR-FTIR spectra of intact ε-PLL and PLL-DDSA(10) are shown in Fig. S2. The bands at 2925 and 2859 cm^{-1}, designated as C-H stretching, were prominent by DDSA introduction. Furthermore, the band at 1540 cm^{-1}, which corresponded to the amide II band from N-H, intensified in the PLL-DDSA(10). Furthermore, the band at 1390 cm^{-1}, designated as methyl C-H bending, appeared in the PLL-DDSA(10). These assignments agreed well with previous literature[22] indicating that efficient modification by DDSA had occurred. Next, we used this prepared polyampholyte for QD conjugation and further analysis.

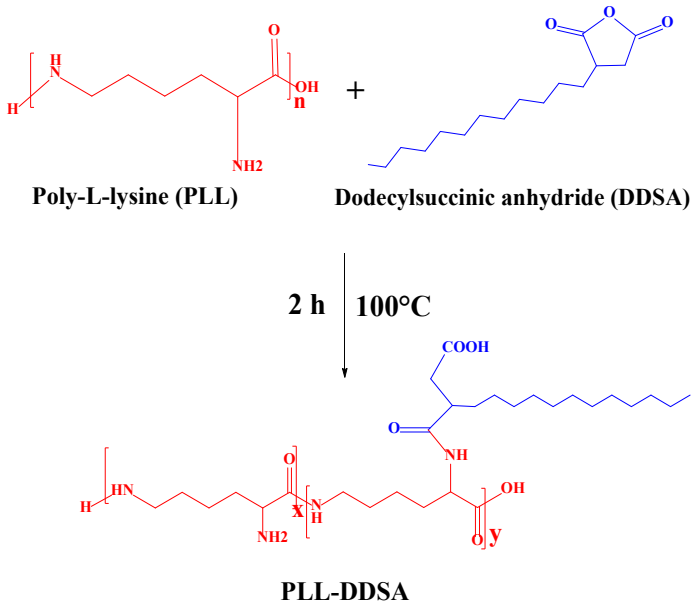

Scheme 2. Preparation of polyampholytes using hydrophobically modified PLL and DDSA.

Characterization of QDs loaded with the hydrophobic polyampholyte

The size and potential of nanomaterials considerably affect the development of nano-therapeutics. In this study, we intended to use a Qdot®streptavidin conjugate to investigate the intracellular delivery using our strategy. The utilized Qdot® streptavidin conjugate is the size of a large macromolecule or protein (approximately 15-20 nm) that has been placed in nanometre-scale crystals of a semiconductor material (CdSe), coated with an additional semiconductor shell (ZnS) to improve the optical properties. This material comprises a biotin-binding protein (streptavidin) covalently attached to a fluorescent label (Qdot® nanocrystal). Accordingly, we characterized the size and potential of bare QDs, bare polyampholytes, and hybrid polyampholyte-QDs. First, we characterized the hydrodynamic diameters; the QDs were approximately 20 nm in diameter. On the other hand, the diameter of PLL-DDSA (10) was 37 nm, whereas, after conjugation of QDs into PLL-DDSA (10), it was in the range of 50 nm (**Fig. 1a**). From TEM images, this increase in the size of PLL-DDSA (10)-QDs suggested a small aggregation of QDs by the electrostatic interaction among QDs and PLL-DDSA(10) (**Fig. 1b and c**). Furthermore, we also investigated the zeta potential of these materials. We observed that the potential of the QDs was -13.0 ± 2.0 mV, whereas it was 13.3 ± 0.6 mV for hydrophobic polyampholytes (PLL-DDSA (10)), and after conjugation with QDs, the potential was 7.9 ± 0.3 mV (Fig. S3). This was indicative of sufficient conjugation of QDs with the hydrophobic polyampholyte PLL-DDSA(10). The electrostatic interaction among QDs and hydrophobic polyampholytes was the main driving force to generate PLL-DDSA (10)-QDs. These results show that a large number of PLL-DDSA particles combine to conjugate with QD particles to form polymer-QDs material complexes. The facilitation of QD delivery relies on the association of polymeric materials such as proteins, peptides, or chemicals, which promotes the interaction of QDs with the plasma membrane and induces internalization via endocytosis. We expect that hydrophobic polyampholytes can be efficiently used to promote intracellular delivery of QDs.

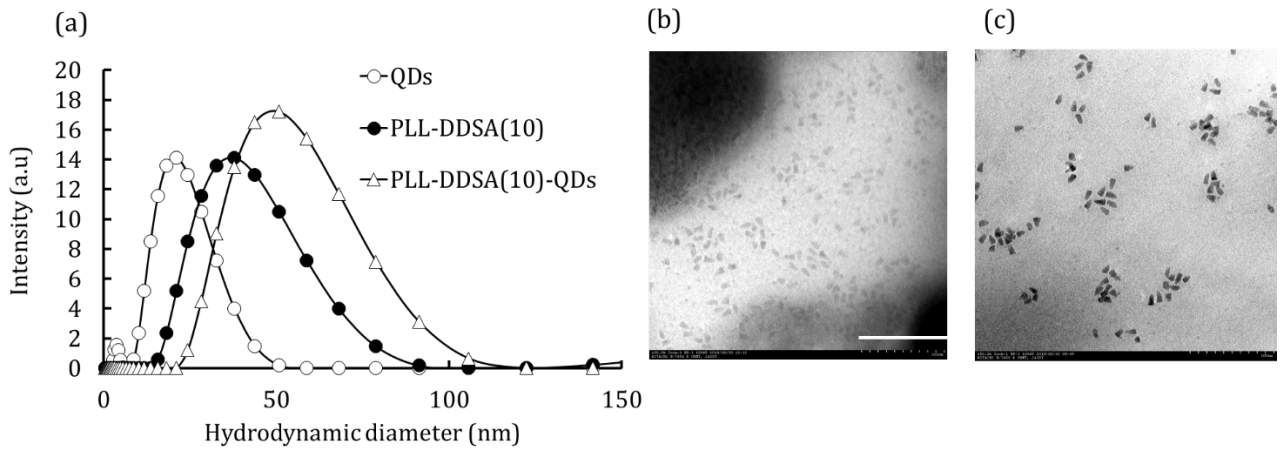

Fig. 1 Assessment of the hydrodynamic diameter of QDs, PLL-DDSA(10), and PLL-DDSA(10)-QDs using DLS analysis at 25 °C and TEM images of (b) QDs and (c) PLL-DDSA(10)-QDs. Scale bar; 100 nm.

The stability of biomaterials is crucial for its practical application. Functionalized QDs have been used effectively for imaging and sensing in living cells; however, stability is critical for improving their usage. **Figure S4** shows that the diameter of Qdot®streptavidin nanoparticles increased continuously from 17.6 ± 4.7 nm to 89.6 ± 26.7 nm in 1 week. On the other hand, the bare hydrophobic polyampholyte PLL-DDSA (10) did not show any drastic change in hydrodynamic diameter, which ranged between 42.7 ±2.4 nm to 59.5 ± 1.6 nm even after 1 week. While conjugation of Qdot®streptavidin nanoparticles with amphiphilic hydrophobic polyampholytes provides colloidal stability, the particle size did not vary significantly but remained constant at around 55 nm. Previously, Choi et al. have shown that organic coated QDs with hydrodynamic diameter < 5.5 nm were excreted rapidly via the renal route, whereas the renal excretion of those with larger diameter (> 15 nm) was prevented and their blood half-life was enhanced by 300-fold and whole half-life by 700-fold. [23] This shows that particles with larger diameter spend more time in circulation and are stable.

Previously, we have shown that the hydrophobic polyampholytes efficiently improve the stability of proteins and genes.[10-13] Another study showed that amphiphilic polymers can be effectively used to provide highly fluorescent QDs that exhibit considerable long-term colloidal stability over a wide range of conditions. [24]

Furthermore, the system should be sufficiently biocompatible for achieving a broad spectrum of biological utility of QDs. Despite significant interest in developing QDs in the medical field, many researchers consider that cadmium containing QDs cannot be used because of their potential cytotoxicity to humans. [25] Therefore, standardization of the dose of QDs by characterizing the uptake concentration is important for reducing the possibility of toxicity. We evaluated the cytotoxicity of QDs using two different cell lines, namely, the L929 fibroblast cells and the RAW 264.7 macrophages. We used streptavidin-conjugated QDs made of semiconductor material (CdSe), which were coated with an additional semiconductor shell (ZnS). We advocate assessing QD exposure to compare the results obtained using two completely different cell lines. Previously, Daok et al. have investigated the uptake and toxicity of CdSe/ZnS QDs by changing cell types.[26]

For the cytotoxicity test, we equated the QD doses in both cell lines. At exposure concentrations between 0 and 5 nM, the QD doses varied negligibly between fibroblasts and macrophages (**Fig. S5a, S5b**). Viability improved for both cell lines when the QD dose was combined with PLL-DDSA (10). This demonstrated that the combination of hydrophobic polyampholytes was not highly cytotoxic. Previously, researchers have used higher concentration of QDs to conduct toxicological studies.[27] At exposure concentrations between 0 and 150 nM, CdS-capped CdSe QDs were more toxic than poly (ethylene glycol)-substituted QDs to the human breast cancer cell line SK-BR-3. On the other hand, when the concentration of the QDs per cell for both bare and poly (ethylene glycol)-substituted QDs was varied, there was no cytotoxic effect in either case.[27]

As we aimed to establish a biocompatible system of QDs with hydrophobic polyampholyte material, we have focused on using lesser amounts of QDs (0 to 5 nM) to inhibit the high intracellular levels of QDs that induce toxicity. The toxicity of PLL-DDSA (10)-QDs was lesser than those of unmodified QDs. Hence, this new hydrophobic polyampholyte has been used to control biocompatibility in this study. When 0.25 nM QDs were combined with PLL-DDSA (10), the viability of the fibroblasts and macrophages were 81% and 85%, respectively. On the other hand, the same concentration of bare QDs showed 71% viability for fibroblasts and 76% for the macrophages. Cell viability decreased to almost 30% at higher concentration (5 nM) of QDs with and without hydrophobic polyampholytes. Hence, we selected 0.25 nM QDs for further investigation.

Adsorption of QD-loaded hydrophobic polyampholytes using the freeze-concentration technology

Previously, we have developed a unique, efficient, sustained, and long-term cell viability approach called freeze-concentration technique for delivery of macromolecules such as proteins and genes. Based on our precedent strategy, we aimed to use the freezing technique for QD internalization and expected the QDs to adsorb onto the cell membrane. Fibroblast L929 cells and RAW 264.7 macrophages were mixed with streptavidin-conjugated QD® 655 combined with hydrophobic polyampholytes (1 mg/mL), followed by cryopreservation in 10% cryoscarless DMSO-free cryoprotectant solution. For this study, we selected streptavidin-conjugated QDs to generate a biocompatible system. Streptavidin was covalently attached on the surface of QDs with highly specific biological activity.

First, we assessed cell viability after treatment with the freezing-concentration technology in the presence of bare QDs, PLL-QDs, and PLL-DDSA (10)-QDs in the cryoprotectant (**Fig. S6**). In all cases, cell viability was more than 80% for both cell lines (L929 and RAW 264.7 cells). Viability was 83% in the presence of bare QDs, and it was 89% in the presence of PLL-QDs; in contrast, high cell viability of 98% was observed in the presence of PLL-DDSA (10)-QDs. This suggested that hydrophobic polyampholytes improved cell viability, which confirmed the results of our earlier study on cryopreservation[28].

Subsequently, we investigated the adsorption of streptavidin-conjugated QDs by treating RAW 264.7 cells with the freezing condition and hydrophobic polyampholytes. Confocal microscopic images showed increased adsorption of QDs after combining PLL-DDSA (10) with the freeze-concentration technique compared to QDs under non-freezing condition (**Fig. 2a, b)**. The increased adsorption of QD-loaded hydrophobic polyampholytes on the cell membrane might be due to the formation of high particle concentration after exclusion of the remaining solution, which resulted in the growth of ice crystals. After thawing, this highly concentrated solution increased interactions with the cell membrane rather than diffusing back to the solution (**Fig. 2b, c**). As a control, we also examined the efficacy of the cell adsorption of bare QDs as well as PLL-QDs without incorporation of the hydrophobic moiety DDSA with or without freeze concentration **(Fig. 2a, b**). Confocal imaging showed few adherences of bare QDs around the cell membrane, with and without the freeze-concentration approach (**Fig. 2c**). In addition, the PLL-loaded QDs showed almost no adsorption under normal as well as freezing condition. The results of quantification also confirmed that a significantly large amount of QDs was incorporated by the cells using PLL-DDSA (10) and the freeze-concentration strategy (**Fig. 2d**). Simultaneously, we checked the adsorption of QDs with or without freezing for normal fibroblast L929 cells, and surprisingly, the QD uptake was not higher than those by RAW 264.7 cells (**Fig. S7a-c**). Furthermore, the results of quantification corroborated those of confocal microscopy (**Fig. S7d**). Interestingly, the majority of QD-encapsulated hydrophobic polyampholytes adsorbed onto the membrane of RAW 264.7 cells compared to that of the control fibroblast L929 cells. We observed remarkable differences in adsorption between each cell type; the uptake of streptavidin-conjugated hydrophobic polyampholytes was stronger in RAW 264.7 macrophages than in normal/healthier L929 cells (**Fig. 2d, S7d**). Many factors may be involved for increasing the interaction of QDs with the cell membrane. Detailed analysis of factors contributing to higher adherence on RAW 264.7 cells, such as the freezing process, specificity of the streptavidin molecule attached to QDs, and hydrophobicity of the carrier should be investigated in the future. Nevertheless, the main objective of this study is the targeted intracellular delivery of QDs on macrophages; in future we will investigate the internalization of QDs by RAW 264.7 cells using our newly developed approach.

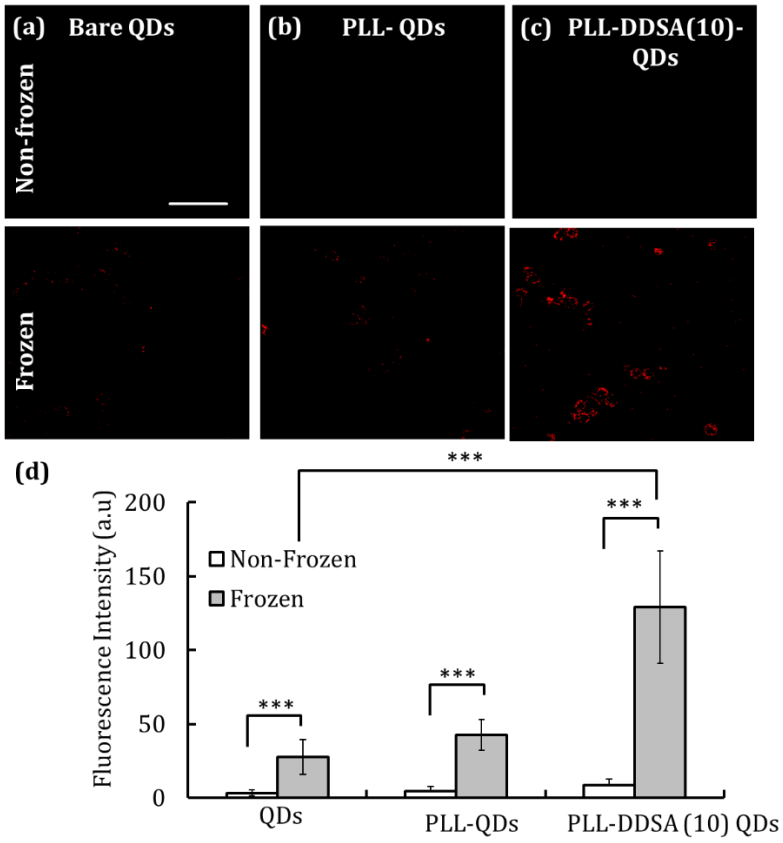

Fig. 2 Confocal images of RAW 264.7 cells showing the adsorption of QDs frozen at –80 °C using 10% cryoprotectant. After 24 h, the cells were thawed at 37 °C and adsorption was investigated using confocal microscopy. Scale bar: 50 µm. (a) Bare QDs, (b) PLL-QDs, and (c) PLL-DDSA (10)-QDs. (d) Mean fluorescence intensity of the adsorbed QDs was determined after freezing using CLSM of RAW 264.7 cells. Data are expressed as the mean ± SD. ***P < 0.001.

Internalization of polyampholyte nanoparticle-conjugated QDs using the freezing method

We investigated the cellular internalization of QDs in RAW 264.7 macrophage during freezing after thawing. The cells and QD-loaded hydrophobic polyampholytes were frozen at –80 °C and thawed at 37 °C, seeded to a glass-bottom dish, and observed using CLSM. As expected, the naked QDs were not transported inside the cells (**Fig. 3a**), and the PLL-loaded QDs also showed the same trend (**Fig. 3b**). However, the use of self-assembled polyampholyte-nanoparticles increased the intracellular delivery of QDs after freezing (**Fig. 3c**). Interestingly, QD transportation was not observed under any condition in the non-frozen state. The amalgamation of freeze concentration methodology and hydrophobic polyampholytes (PLL-DDSA (10)) promoted the delivery of QDs **(Fig. 3a-c**). According to our previous studies, the unique combination of self-assembled polyampholyte nanoparticles and freeze-concentration was also useful for protein and gene delivery.[10-15] These results might be due to the escalation in particle concentration, which increased interactions with the cell membrane in the frozen system and guided efficient adsorption of the materials and subsequent cytoplasmic internalization. However, it is important to further understand the effect of factors affecting the intake of QD particles on cellular internalization dynamics associated with this blending of methods. Previously, Kelf et al. have reported QD internalization via non-specific endocytosis.[29] They highlighted that the uptake mechanism was largely initiated by surface receptor interactions between charged particles, involvement of receptors, or protein modification on the materials. [30] We believe that the non-specific binding of QDs to the cell membrane might be due to the hydrophobic and cationic factor in the polyampholytes and freezing stress, which plays

important roles in the non-specific adsorption and entry via endocytosis[31, 32].

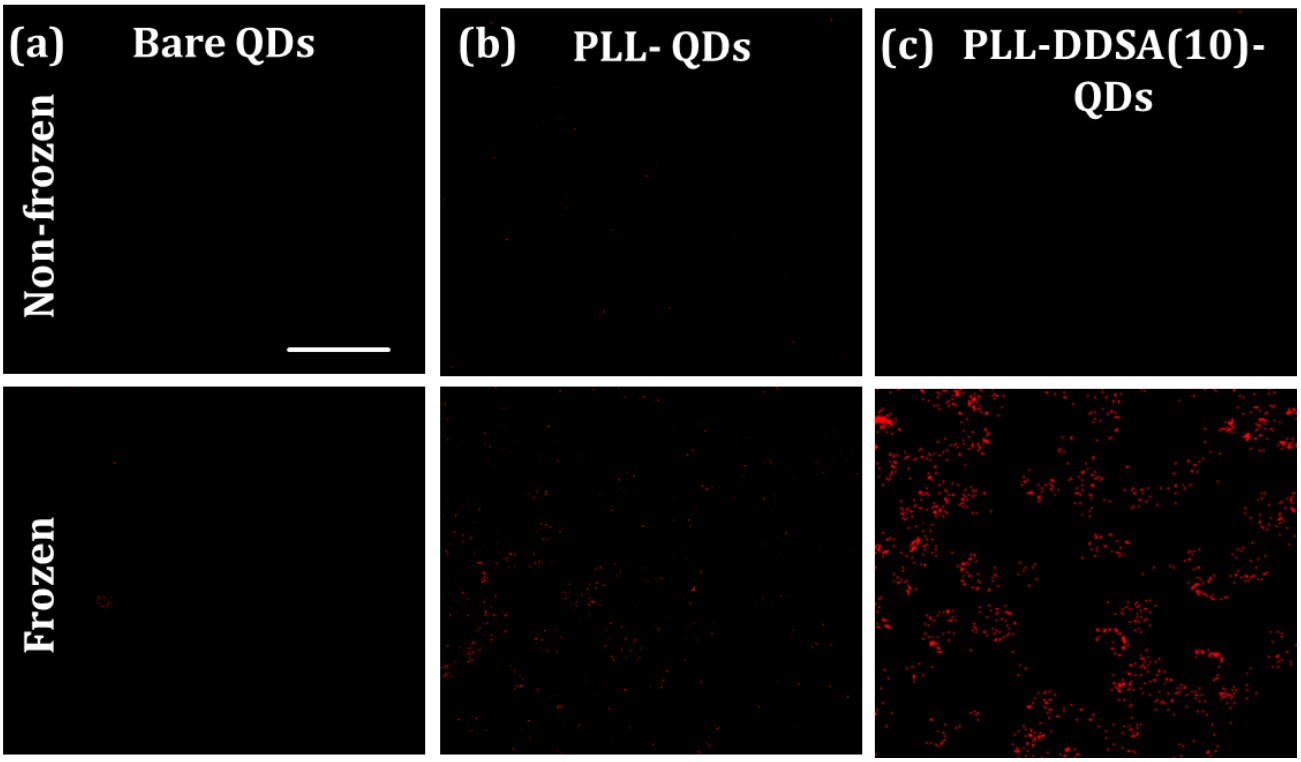

Fig. 3 Internalization of QDs in RAW 264.7 cells. RAW 264.7 cells (1 x 10^6 cells/mL) were cryopreserved with 10% cryoprotectant and PLL or PLL-DDSA (10)-QDs at −80°C. The cells were thawed and seeded for 24 h at 37°C. (a) Bare QDs, (b) PLL-QDs, and (c) PLL-DDSA(10)-QDs. Scale bar: 50 µm.

Several physical methods such as electroporation[6], sonication[33], and microinjection[34] have been used for transportation of QDs into the cell cytoplasm. These techniques have been used to successfully inject QDs and induce penetration of these materials (QDs) in the cell membrane in large quantities. However, the presence of strong electric field and energy creates lethal nano-pores in the membrane, which disrupt cellular homeostasis and lead to loss of cell viability.[35] Recently, osmotic lysis was developed for intracellular delivery of particles encompassed in pinocytic vesicles. Nelson et al. used osmotic lysis for intracellular delivery of QD-myosin conjugate in COS 7 cells.[36] However, this technique is time-consuming and cytoplasmic internalization is difficult to achieve. Our freezing technique is simple, less time-consuming, and allows non-specific imaging of extracellular and intracellular proteins and organelles.

Endosomal escape of QDs from polyampholyte nanoparticles

Materials are transported to reach their destined compartment inside cells for implementing particular functions. A major drawback is the difficulty in efficient cytoplasmic delivery of QDs even after their entry and penetration inside the cells. The main problem is the inability of materials to be released from endosomes after being engulfed in endocytic vesicles. Previously, cell-penetrating peptides such as TAT and polyarginine were used to deliver QDs into the cytoplasm; however, QDs are trapped in endosomes, and their release from this compartment is difficult.[37,38] In our study, we observed sufficient internalization of QDs in RAW 264.7 cells using the freezing method (**Fig. 3c**). It is important to decipher the intracellular co-localization events in which QDs and organelle tracking dyes are co-delivered into living cells when freezing drives the internalization. To observe the intracellular distribution of QDs after freezing, the thawed RAW 264.7 cell suspensions were seeded into plates and cultured for 24 h. We used CLSM to observe the localization of streptavidin-conjugated QD 655; endosomes were labelled with LysoTracker Green, while cell nuclei were stained with Hoechst 33342. In control experiments, neither bare QDs nor PLL-loaded QDs alone showed release of QD material **(Fig. 4a, b**). However, efficient release of QDs was visible in the CLSM images, which clearly indicated the cytosolic release of materials with the combination of hydrophobic polyampholytes and the freezing system (**Fig. 4c**). The insufficient release from endosomes is possibly because of the strong binding of PLL-QDs, which leads to the formation of a stable complex that is difficult to dissociate. The delivery of free QDs into the cytosol is essential for studying intracellular molecules and structures. Wagner et al. have developed dimethyl maleic acid-melittin derivative-PLL, which shows pH-triggered endosomolytic activity for enhanced gene function[39]. Shi et al. demonstrated the release of insulin using a pH-sensitive grafted

amphipathic polymer composed of N-tocopheryl-N'-succinyl-ε-poly-L-lysine, which contains hydrophobic alkane and ionisable carboxyl branches.[40] Previously, we have shown that the pH responsiveness of this polymer with long hydrophobic pendant groups anchored into the liposomes improved the ability of liposomes to disrupt lipid bilayers. In our previous study, hydrophobic polyampholyte-modified liposomes also induced the endosomal escape of lysozyme as well as ovalbumin[13]. The undissociated forms of the carboxylic moieties are prevalent at low pH, which leads to enhanced hydrophobic interactions and subsequent release of QDs. Possibly, the presence of both ionisable entities and long alkyl chain can induce aggregation via hydrophobic interaction. Our present findings are in good agreement with our previous results. Upon endocytosis, low pH in the endosomes results in the release of QDs into the cytoplasm. Owing to this pH sensitivity factor, the hydrophobic polyampholyte system releases QDs more efficiently than bare PLL.

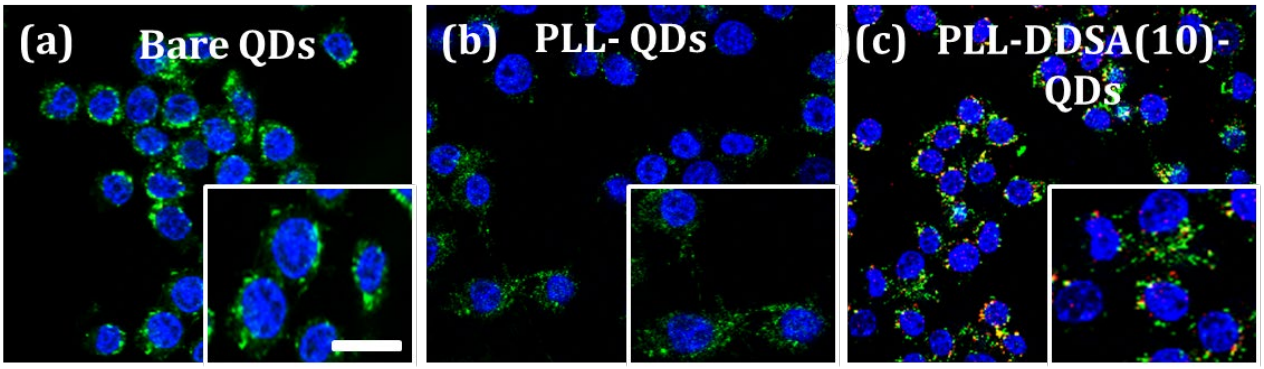

Fig. 4 Endosomal escape of QDs in RAW 264.7 cells. RAW 264.7 cells (1 x 10^6 cells/mL) were cryopreserved with cryoprotectant and PLL or PLL-DDSA (10)-QDs at −80°C. The cells were thawed and seeded for 24 h at 37 °C. The late endosomes and nuclei were stained with Lysotracker Green and Hoechst blue 33342, respectively. (a) Bare QDs, (b) PLL-QDs, and (c) PLL-DDSA(10)-QDs. Scale bar: 10 µm.

Conclusion

In this study, the previously developed freeze-concentration method was used to internalize QD-conjugated hydrophobic polyampholyte complexes, which can be utilised for long-term live-cell imaging. In particular, the hydrophobic polyampholyte-QDs were prepared by mixing the polymer with the less-toxic semiconductor QD materials, which were efficiently internalized in the macrophage cytoplasm. Furthermore, the efficient endosomal escape of QDs caused by the hydrophobic polyampholytes at acidic pH increases the chances of cytoplasmic delivery. We conclude that the freeze-concentration strategy increases internalization and efficient endosomal escape of QDs, which is essential for the utilization of materials for biological diagnosis.

Conflicts of interest

There are no conflicts to declare.

Acknowledgements

This study was supported in part by a Grant-in-Aid, KAKENHI (16K12895), for scientific research from Japan Society for the Promotion of Science.
We would like to thank Editage (www.editage.com) for English language editing.

References

1. E. Derivery, E. Bartolami, S. Matile and M. Gonzalez-Gaitan, *J. Am. Chem. Soc.,* 2017, **139**, 10172-10175.
2. V, Morosini, T. Bastogne, C. Frochot, R, Schneider, A. Francois, F. Guillemin and M. Barberi-Heyob, *Photochem. Photobiol. Sci.,* 2011, **10**, 842-851.
3. B. Cedric, M. Mathieu, T. Antoine and D. Maxime, *Proc. Natl. Acad. Sci. U.S.A.,* 2007, **104**, 11251-11256.
4. I. Chung, R. Akita, R. Vandlen, D. Toomre, J. Schlessinger and I. Mellman, *Nature* 2010. **464**, 783-787.
5. L. Qi and X. Gao, *ACS Nano*, 2008, **2**, 1403-1410.
6. C. Sun, Z. Cao, M. Wu and C. Lu, *Anal. Chem*., 2014, **86**, 11403-11409.
7. W. S. Meaking, J. Edgerton, C. W. Wharton and R. A. Meldrum, *Biochim. Biophys. Acta*., 1995, **1264**, 357-362.
8. X. Zhao, Y. Wu, D. Gallego-Perez, K. J. Kwak, C. Gupta, X. Quyang and L. J. Lee, *Anal. Chem*., 2015, **87**, 3208-3215.
9. C. E. Probst, P. Zrazhevskiy, V. Bagalkot and X. Gao, *Adv. Drug Deliv. Rev.*, 2013, **65**, 703-718.
10. S. Ahmed, F. Hayashi, T. Nagashima and K. Matsumura, *Biomaterials,* 2014, **35**, 6508−6518.

11. S. Ahmed, S. Fujita and K. Matsumura, *Nanoscale,* 2016, **8**, 15888−15901.
12. S. Ahmed, T. Nakaji-Hirabayashi, T. Watanabe, T. Hohsaka and K. Matsumura, *ACS Biomater. Sci. Eng*., 2017, **3**, 1677−1689
13. S. Ahmed, S. Fujita and K. Matsumura, *Adv. Heathc. Mater*., 2017, **6**, 1700207.
14. S. Ahmed, O. Miyawaki and K. Matsumura, *Langmuir*, 2018, **34**, 2352-2362.
15. S. Ahmed, K. Okuma and K. Matsumura, *Biomater. Sci.,* 2018, **6**, 1791-1799.
16. C. Jones and D. W. Grainger, *Adv. Drug Deliv. Rev*., 2009, **61**, 438-456.
17. P. Ponomarev, *Mol. Imaging Biol.,* 2017, **19**, 379-384.
18. D. Hirayama, D. Iida and H. Nakase, *Int. J. Mol. Sci*., 2018, **19**, 92.
19. H. Cui, J. Fang, Z. Zuo, J. Deng, Y. Li, X. Wang and L. Zhao, *Oncotarget*, 2017, **9**, 7204-7218.
20. K. Ishihara, W. Chen, Y. Liu, Y. Tsukamoto and Y. Inoue, *Sci. Technol. Adv. Mater*., 2016, **17**, 300-312.
21. T. Fukui, H. Kobayashi, U. Hasegawa, T. Nagasawa, K. Akiyoshi and I. Ishikawa, *Drug Metab. Lett*., 2007, **1**, 131-135.
22. H. Yu, Y. Huang and Q. Huang, *J. Agric. Food Chem.*, 2010, **58**, 1290-1295.
23. H. S. Choi, W. Liu, P. Misra, E. Tanaka, J. P. Zimmer, B. I. Ipe, M. G. Bawendi and J. V. Frangioini, *Nat. Biotechnol*., 2007, **25**, 1165-1170.
24. W. Wang, A. Kapur, X. Ji, M. Safi, G. Palui, V. Palomo, P. E. Dawson and H. Mattoussi, *J. Am. Chem. Soc.*, 2015, **137**, 5438-5451.
25. J. Wang, R. Liu and B. Liu, *Mini Rev. Med. Chem.,* 2026, **16**, 905-916.
26. B. B. Manshian, S. J. Soenen, A. Ali, A. Brown, N. Hondow, J. Wills, G. J. S. Jenkins and S. H. Doak, *Toxicol. Sci*., 2015, **144**, 246-258.
27. E. Chang, N. Thekkek, W. W. Yu, V. L. Colvin and R. Drezek, *Small*, 2006, **2**, 1412-1417.
28. R. Rajan, F. Hayashi, T. Nagashima and K. Matsumura, *Biomacromolecules*, 2016, **17**, 1882-1893.
29. T. A. Kelf, V. K. A. Sreenivasan, J. Sun, E. J. Kim, E. M. Goldys and A. V. Zvyagin, *Nanotechnology,* 2010, **21**, 1-8.
30. J. Reiman, V. Oberle, I. S. Zuhorn and D. Hoekstra, *Biochem. J.*, 2004, **377**, 159-169.
31. L. Chen, J. M. Mccrate, J. CM. Leeand H. Li, *Nanotechnology*, 2011, **22**, 105708.
32. A. Nan, X. Bai, S. J. Son, S. B. Lee and H. Ghandehari, *Nano Lett.,* 2008, **8**, 2150-2154.
33. Z. Fahmi and J. Y. Chang, *Procedia Chem.,* 2016, **18**, 112-121.
34. L. Damalakiene, V. Karabanovas, S. Bagdonas, M. Valius and R. Rotomskis, *Int. J. Nanomedicine*, 2013, **8**, 555-568.
35. S. Majid, E. C. Yusko, Y. N. Billeh, M. X. Macrae, J. Yang and M. Mayer, *Curr. Opin. Biotechnol.*, 2010, **21**, 439.
36. S. R. Nelson, M. Y. Ali, K. M. Trybus and D. M. Warshaw, *Biophys. J.,* 2009, **97**, 509-518.
37. B. C. Lagerholm, M. Wang, L. A. Ernst, D. H. Ly, H. Liu, M. P. Bruchez and A. S. Waggoner, *Nano Lett.*, 2019, **4**, 2004
38. J. B. Delehanty, I. L. Medintz, T. Pons, F. M. Brunel, P. E. Dawson and H. Mattoussi, *Bioconjugate Chem*., 2006, **17**, 920.
39. M. Meyer, A. Zintchenko, M. Ogris and E. Wagner, *J. Gene Med.*, 2007, **9**, 797-805.
40. Y. Fang, J. Xue, L. Ke, Y. Liu and K. Shi, *Drug Deliv.*, 2016, **23**, 3582-3593.

Electronic Supplementary Information (ESI) for

Cytosolic delivery of quantum dots mediated by freezing and hydrophobic polyampholytes in RAW 264.7 cells

Sana Ahmed[a, b], Tadashi Nakaji-Hirabayashi[b, c], Robin Rajan[a], Dandan Zhao[a] and Kazuaki Matsumura*[a]

[a]School of Materials Science, Japan Advanced Institute of Science and Technology (JAIST), Nomi, Ishikawa 923-1292, Japan E-mail: mkazuaki@jaist.ac.jp

[b]Graduate School of Science and Engineering, University of Toyama, 3190 Gofuku, Toyama, Toyama 930-8555, Japan

[c]Graduate School of Innovative Life Science, University of Toyama, 3190 Gofuku, Toyama, Toyama 930-8555, Japan

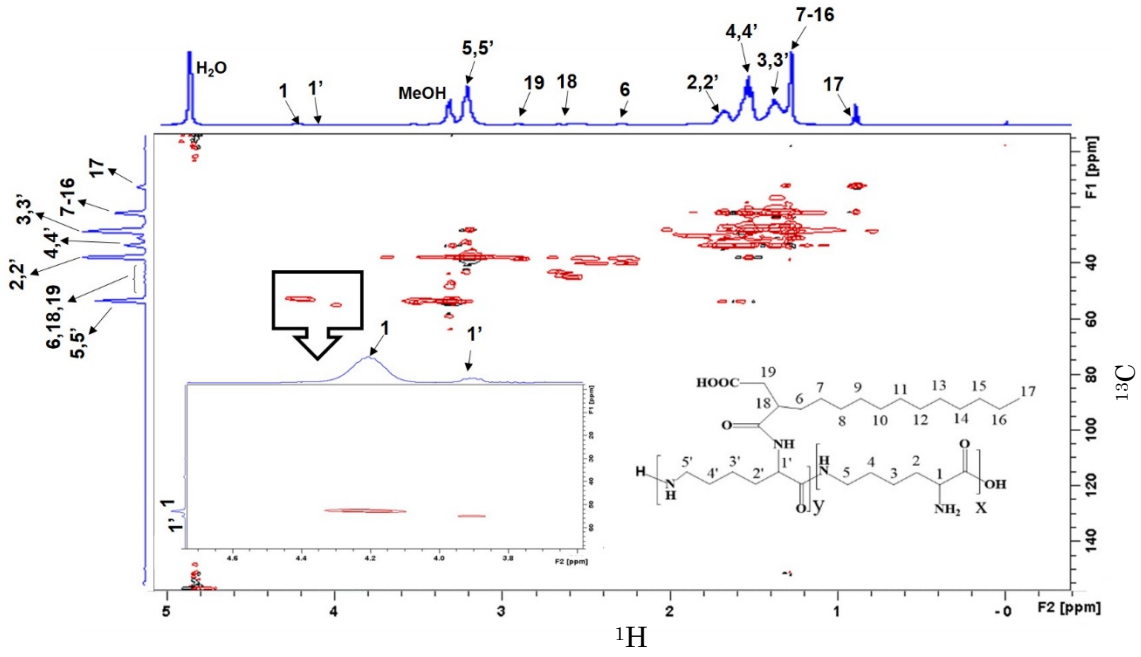

Fig. S1 NMR signal assignment of PLL-DDSA(10) in methanol-d_4.

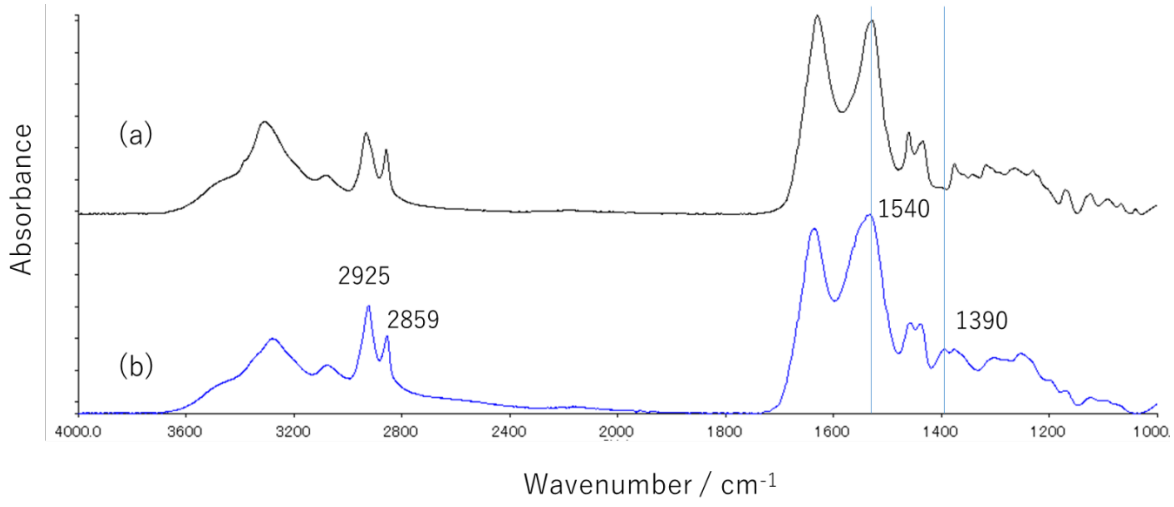

Fig. S2 ATR-FTIR spectra of (a) ε-PLL and (b) PLL-DDSA(10).

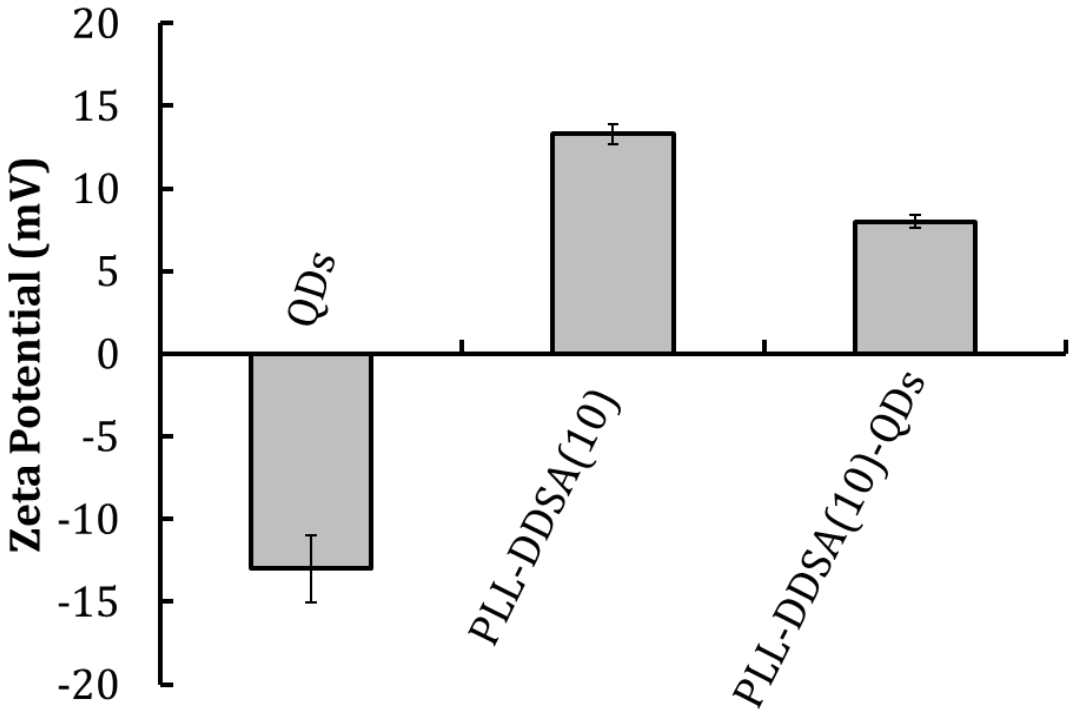

Fig. S3 Zeta potential of QDs, PLL-DDSA(10), and PLL-DDSA(10)-QDs determined using DLS . Data are expressed as mean ± SD.

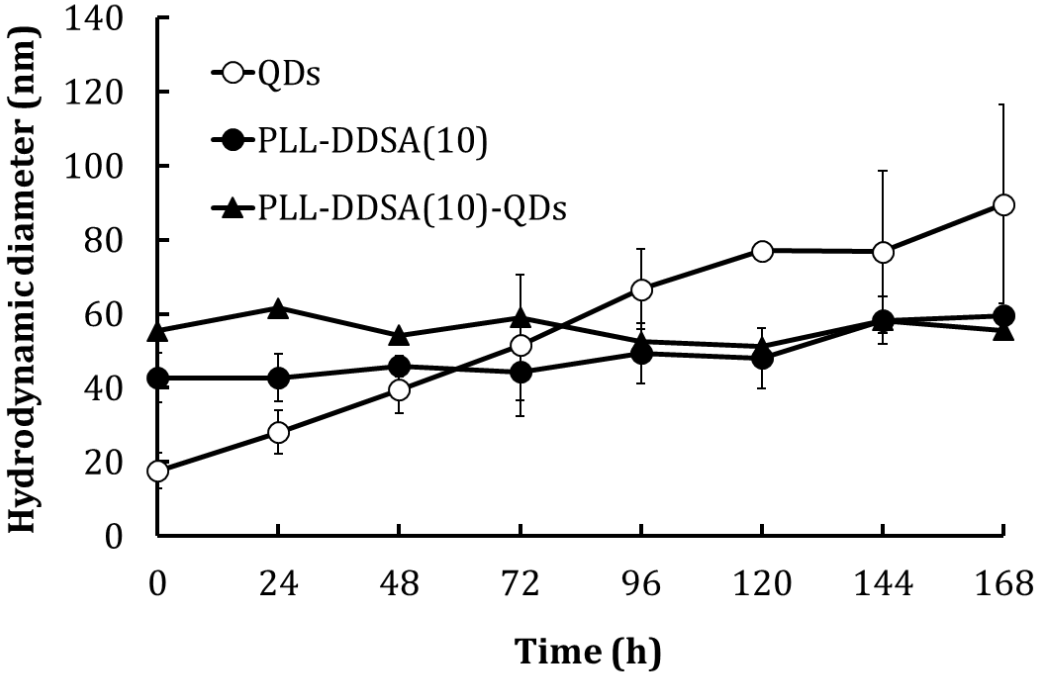

Fig. S4 Particle size stability of QDs only and PLL-DDSA(10)-QDs over 7 days at 25 °C. Data are expressed as mean ± SD.

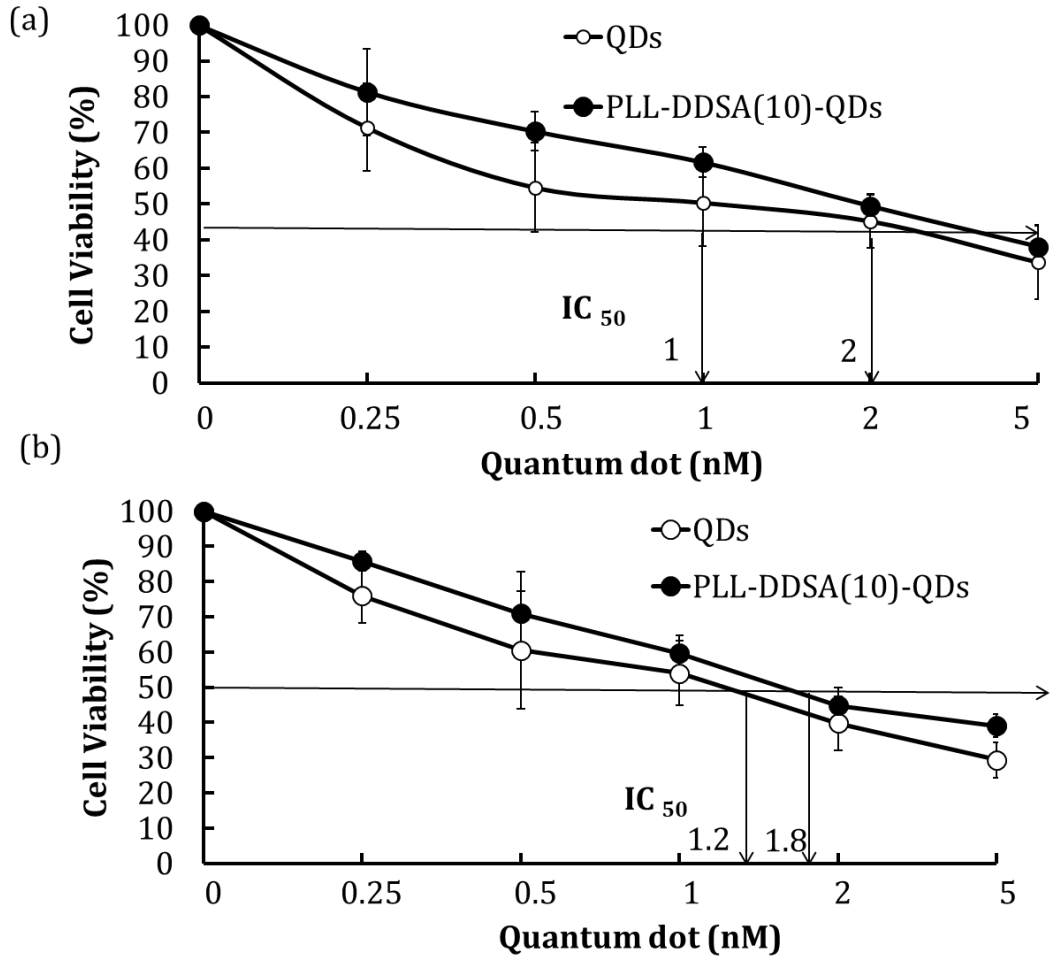

Fig. S5 Cytotoxicity of QDs alone and PLL-DDSA(10)-QDs in fibroblast L929 cells and RAW 264.7 macrophages. The cells were incubated with different concentration of QDs for 48 h and analysed using MTT. The polyampholyte concentration was fixed, whereas the quantum dot concentration varied from 0 to 5 nM. IC_{50} represents the concentration of QDs that caused a 50% reduction in the number of treated cells compared to the untreated control. (a) Fibroblast L929 cells and (b) RAW 264.7 macrophages. Data are expressed as mean ± SD.

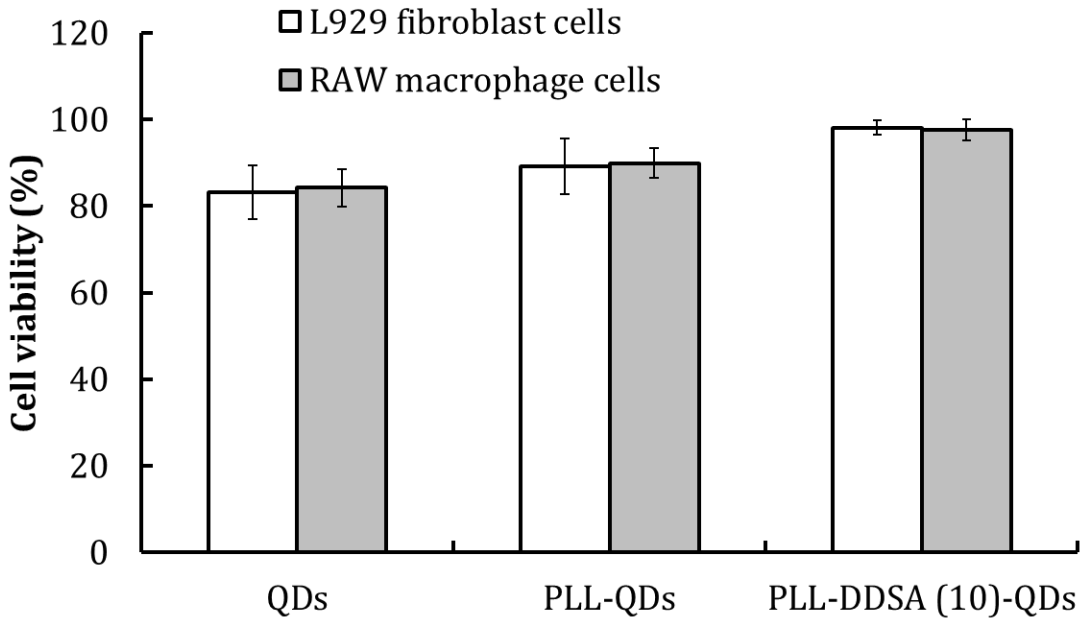

Fig. S6 Cell viability in the presence of QDs alone or QD complexes with PLL and PLL-DDSA (10) in the presence of a cryoprotectant. Data are expressed as mean ± SD.

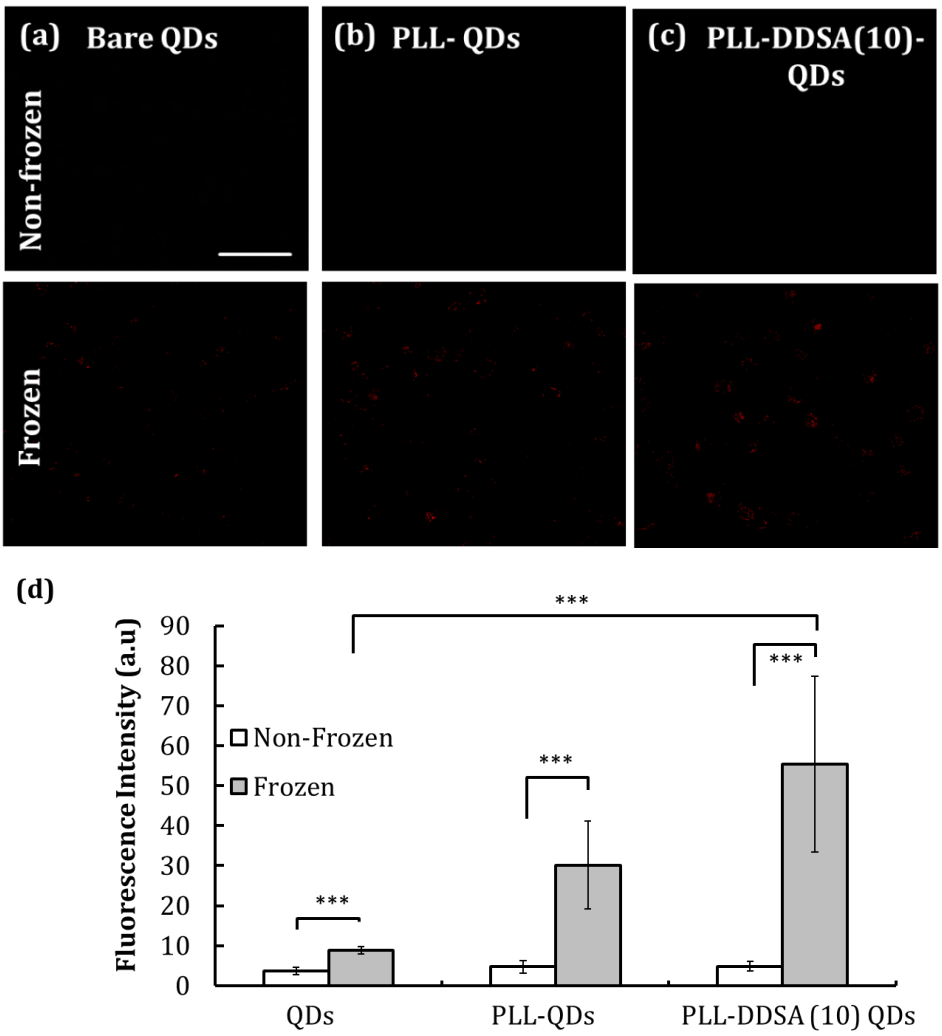

Fig. S7 Confocal images of L929 fibroblast cells showing the adsorption of QDs after being frozen at -80 °C in a cryoprotectant. After 24 h, the cells were thawed at 37 °C and the adsorption was investigated using confocal microscopy. Scale bar: 50 μm. The panels show the (a) bare QDs, (b) PLL-QDs, and the (c) PLL-DDSA(10)-QDs. (d) Mean fluorescence intensity of the adsorbed QDs was determined after freezing using CLSM of RAW 264.7 cells. Data are expressed as the mean ± SD. ***$P < 0.001$.